

A Numerical Comparison between Aluminum Alloy and Mild Steel in Order to Enhance the Energy Absorption Capacity of the Thin Walled Tubes

Jamal O. Sameer, Omar S. Zaroog, Samer F., Abdulbasit Abdullah

Abstract— the current study describes and comparison between the behavior of the thin wall rectangular tube cross- sections modeled by mild steel and aluminum alloy, subjected to dynamic compression load. We examine the reaction of the tube of various thicknesses and materials (mild steel A36 and aluminium alloy AA6060), subjected to direct and oblique loading. The study investigates the behavior of the rectangular tube, with various weights of various hollow aluminum foam. The choice of the best design of tube parameter is based on the method called multi criteria decision making (MCDM). The examined criteria are the peak force, crush force efficiency (CFE), how also the energy absorption in case of oblique and direct load. The optimal choice of the rectangular tube is the aluminium rectangular profile of 3.4 mm thickness and hollow aluminium foam type ($E= 0.652\text{Kg}$), under oblique load, with enhancement of the energy absorption of 11.2 %, an improvement of CFE by 42.3%, decrease of peak force by 30.7 %. In case the direct load, the enhancement of the energy absorption of 7.2 %, an improvement of CFE by 88%, decrease of peak force by 39.7 %. The aim of using thinner tube and hollow aluminium foam is to keep the final design the lowest possible weight, to improve the CFE and the energy absorber capacities in order to attain higher passenger safety.

Index Terms— aluminum alloy, mild steel, dynamic compression, thin wall, energy absorption, aluminum foam

I. INTRODUCTION

Crashworthiness has become one of the basic properties in the protection of passengers and being so, no one can ignore its essential role while designing any kind of vehicle. This is the feature that provides security by absorbing crash and defending travelers at the moment of the accident. The significance of the crashworthiness in both land and air transportation has been already recognized and a certain emphasis to its further development has been given. Crashworthiness basically means reducing damage, obtaining a higher degree of safety by absorbing the unexpectedly, suddenly created energy. In order to achieve the protection of the passengers in the dangerous moment of a crash, vehicle has to be designed in a manner to provide

Manuscript Received on November , 2014.

Jamal O. Sameer, Univirsiti of Tenaga Nasional/ College of Engineering, Kuala Lumpur, Malaysia.

Omar S. Zaroog, Mechanical Engineer, He is currently an Dr. lecturer at Univirsiti of Tenaga Nassional / College of Engineering / Kuala Lumpur, Malaysia.

Samer F., Mechanical Engineer, He is currently an Dr. lecturer at Alanbar University/ Engineering/, Alanbar-Ramadi, Iraq.

Abdulbasit Abdullah, Mechanical Engineer, Univirsiti of Tenaga Nassional / College of Engineering / Kuala Lumpur, Malaysia.

structural integrity which defends passengers by transforming the kinetic energy caused by quick increase or decrease of speed into other forms of energy. Recently the metallic foams have been significantly developed and this has opened new opportunities in the impact engineering. Properties, like high energy absorption capability at very lightweight, high specific rigidity, constant distortion mode, and good adaptation to the distortion, etc. provide the necessary features for their application [1, 2]. Due to the promising properties of these materials, thin-walled structures filled with cells or foamed materials, subjected to impact loads in the frontal longitudinal structures, have become subject of further researches [3–9]. The energy absorption capability of the metallic foam materials has been approved by the studies. The complete numerical, and experimental research of Hanssen et al. [10–14] regarding the thin-walled aluminium columns with foam filling, subjected to direct load, contributed to the better understanding of the aluminium foam materials. The results confirmed that the usage of foam-filler materials considerably increases not only the capacities of the thin wall profiles in absorbing the energy, but also the crush force. Hanssen et al. [14] solved a mass minimization question of the foam material properties, including the energy absorption capability, the force, and the stability of the aluminium columns of squared shape. They displayed – making use of a graphical analysis- the manifestation of the various crashworthiness dimensions. Song et al. [15] similarly proved the relation between the usage of foam-filler materials in the thin-walled structure and its increased energy absorption capability. The results confirm that the filler materials and the geometry of the tube need to be taken simultaneously in consideration in order to detect the ideal design. Chen [16] based empirical studies also on the mass minimization in order to investigate the crashworthiness features of the foam-filled tubes subjected to huge twisting rotational load. Afterwards Chen et al. [17] – with the help of the curve fitting technique - investigated the bending crush, in order to find the lowest possible weight with the required energy absorption capabilities and bending stiffness restrains. The main purpose of the research of Nariman-Zadeh et al. [18], was to obtain –with the usage of a multi objective genetic algorithm- the lowest possible weight, and in the same time the highest possible energy absorption capacities.

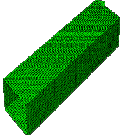
A Numerical Comparison between Aluminum Alloy And Mild Steel in Order to Enhance the Energy Absorption Capacity of the Thin Walled Tubes

Zarei and Kroger [19,20] also used the multi-design optimization (MDO) for the geometric constraints of the profiles with foam filling, as base for their experimental examination. The various researches focused mainly on the improvement of the experiential models of the foam-filled structures and their crashworthiness properties, while haven't been given attention to their design optimization. Moreover, based on the study of Nariman-Zadeh et al. [18], the above mentioned design optimization should be processed in a multi objective framework, focusing on the effect of the various crashworthiness indicators on each other. The purpose of the current study is to optimize the rectangular, aluminium foam filled thin-walled tube in case of for single and multiple crashworthiness indicators, and to improve their crashworthiness capabilities.

II. DESIGN METHODOLOGY

The study examines and comparison the behaviour of the cross sectional, thin wall, rectangular mild steel and aluminium alloy profile. The profile is long 350mm, thick 1, 1.2, 1.3 and 2 mm, in case of mild steel and 1.5, 2, 3 and 3.4 mm, in case of aluminium alloy, with perimeters of 300 mm. As a first step, we survey the crashworthiness properties of the cross sectional profiles, and this is followed by the research of their improvement possibilities and the choice of the optimal design. The rectangular profile of various weights is filled with hollow aluminium foam of 540kg/m³ density, and is subjected to direct and oblique (30 degrees) impact load. The simulation is based on an impact mass of the 25% of the total weight of the vehicle; with an initial speed of 54km/hr. Table 1 illustrates the various profiles.

Table 1: Profile dimensions and geometry examined in the current study

Profile	Specimen ID	Perimeter mm	Length mm	Major Dimension mm	Minor Dimension mm	Thickness mm	Shape
Rectangular	R-300	300	350	90	60	1	
						1.2	
						1.3	
						1.5	
						2	
						3	
						3.4	

A. Force max and Peak load

The maximum force means the supreme impact, and the deformation that the members of the passenger car can absorb, maintaining the passenger cabin safe. The goal to achieve is to have vehicle members able to absorb the low-energy and low-velocity mass loads without constant deformation of the structure [21].

B. Energy Absorption

In Figure 1 the load-displacement curve illustrates the

design of the energy absorption (EA) and its calculation.

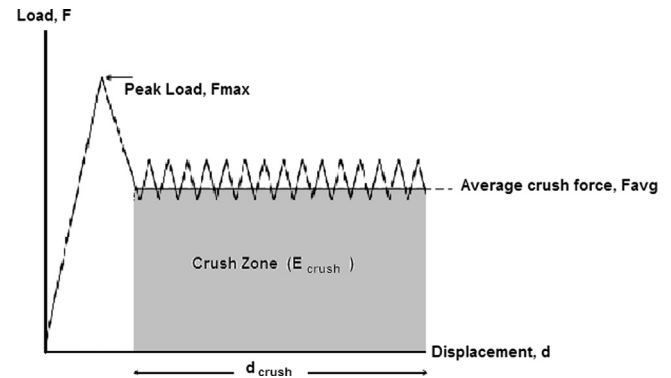


Fig.1. Force displacement characteristics [40]

$$EA = \int_0^{\delta b} P.d \delta \quad (1)$$

P stands for the direct crush force; δ is for the deformation length of the crush, like in the calculation (1).

$$EA = \int_0^{\delta b} P.d \delta = P_m (\delta b - \delta i) \quad (2)$$

P_m is stands for the crushing load; δi for the original length of the crushing specimen. The ideal energy absorption –once reached it- should maintain the maximum force for the whole length of the deformation.

C. Crush Force Efficiency, CFE

The CFE is the main crush force (P mean) divided by the peak crush load (P peak) as follows

$$CFE = \frac{P_{mean}}{P_{peak}} \quad (3)$$

Based on the crash force efficiency (CFE) we can estimate the energy absorption capacities [22]. The value of CFE is computed by dividing the average value of force with the load-displacement curve on the peak force at the moment of the impact [23]. The goal is to keep the CFE at a high value, as its low value would mean high peak force and decreased passenger safety. The CFE indicates the effectiveness of the passenger car's structure, in case of an impact [24]. The required high CFE and low peak load values can be obtained by using the trigger mechanism [25] or by the usage of a thicker wall of the tube.

III. DYNAMIC ANALYSIS

The tests in the current study are performed by the software of ABAQUS/Explicit version 6.10, as finite element method, to reproduce the profile's performance in case of energy absorber members in the longitudinal frontal members of the vehicle in case of direct, and oblique dynamic load. The software program is appropriate to simulate various procedures of computational fluid dynamics (CFD) or standard/ electrical model and in the same time it saves time, energy, and investment comparing to the implicit methods. It has the same abilities with the implicit methods in order to

simulate identical circumstances of high speed dynamic, and impact load [26], and this makes it suitable to examine the effects of direct and oblique loads, and of the energy absorption capacity.

A. Finite Element Modeling

The below equation can be used in order to locate a point in a continuum:

$$\sigma_{ij} + f_i = \rho \ddot{X}_i \quad (4)$$

or

σ_{ij} stands for the stress, ρ the density, f_i for the body force and \ddot{X}_i for the acceleration. Eq. (13) can be utilized in case of simulated work by the usage of the divergence theorem:

$$\int_V \rho \ddot{X}_i dV + \int_V \sigma_{ij} \delta X_{i,j} dV - \int_V \rho f_i \delta X_i dV - \int_{S^2} t_i \delta X_i dS = 0 \quad (5)$$

In terms of the matrix form:

$$\sum_{i=1}^n \left\{ \int_V \rho N^i N^i dv + \int_V B^i \sigma dv - \int_V \rho N^i b dv - \int_A N^i F dA + \int_S N^i F_c ds \right\}^i = 0 \quad (6)$$

In the equation n stands for the sum of components, σ for the stress column vector, N for the interpolation matrix, a for the nodal acceleration column vector, B for the strain matrix, b for the body load column vector, and F for the applied traction load (in case is applicable).

A more common explanation of this is shown below:

$$[M] \left[\frac{d^2 u}{dt^2} \right] + [C] \left[\frac{du}{dt} \right] + [K] \{U\} = [F(t)] \quad (7)$$

M stands for mass matrix, C for damping matrix and K for stiffness matrix. The calculation of the displacements is followed by the computation of contact forces, internal and kinetic energies, and plastic strains. In case of nonlinear dynamic issues, like the impact, is desired to have explicit finite element software providing central difference method. The explicit method is able to separate the total length of time in minor time periods, called time increments. The dynamic equilibrium calculation (see Equation 1) is explained and variables are specified at $(t+\Delta t)$ in base of the time value they have at time t . The explicit techniques provide the information at the time period $n+1$ based on the preceding time period (n) and without depending on the present time period, contrary to the implicit methods, where the time period $n+1$ is depends on the preceding, plus the present time period (n). In the current research, (FE) models illustrating the profiles, with and without foam filling, has been used by ABAQUS Explicit, in order to forecast the behaviour of the thin wall structures in case of falling impinging mass. The thin wall tube was modeled by the usage of 4 node shell continuum (S4R) elements and with 5 integration points in the length of the thickness way of the component. The foam has been modeled by the usage of 8-noded continuum components and diminished incorporation techniques, to evade volumetric locking, combined with the hourglass control, in

order to evade artificial zero energy distortion. The size of the shells and foam elements is 5 mm, to guarantee an adequate mesh density to observe the distortion procedure. The “general contact algorithm” was chosen to simulate contact interaction among the components, and to evade interpenetration of the tube wall. The computational time of the current algorithm is less intensive. Connections among the empty and foam filled tube wall are modeled as finite sliding penalty based contact algorithm with hard contact and contact pairs. The rate of the friction coefficient for the interfaces is 0.2 [29, 30, and 32]. The striker, with impact speed of 15 m/s (56 km/h), and with compactor load of 275 kg, is modeled as a rigid body, having one translational displacement, and in the same time the rest of the translational and rotations degree are stable (Fig. 2).

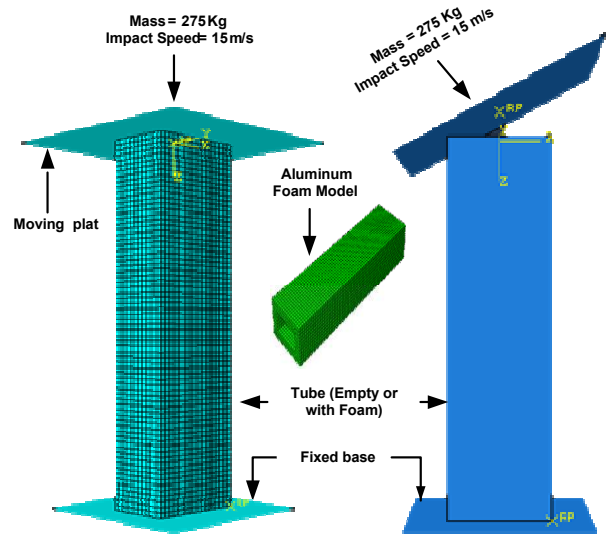


Fig.2. Design of frontal longitudinal members

The impact velocity is based on the New Car Assessment Program (NCAP) with a mass of 25% of a vehicle (1100 kg). All the energy absorbing tubes are of A36 steel material, which is supposed to absorb the kinetic energy of 275 kg mass, as in natural conditions the supreme energy absorbed by two tubes is minor than 50% [30]. The classification of the A36 steel is based on the constitutive isotropic hardening model of Johnson–Cook, which considers the ratio of the strain effects and hardening, and is appropriate in cases with a big range of strain rate variety and temperature changes produced by the thermal softening [33]. The above features are shown in Eq. (3) [34]:

$$\sigma_T = \left[A + B (\epsilon_{eff}^p)^N \right] \left[1 + C \ln \frac{\dot{\epsilon}_{eff}^p}{\dot{\epsilon}_0} \right] \left[1 - \left(\frac{T - T_0}{T_{melt} - T_0} \right)^M \right] \quad (8)$$

σ_T stands for the flow stress in dynamic circumstances, ϵ_{eff}^p for the effects of the plastic strain, $\dot{\epsilon}_{eff}^p$ for the effective plastic strain rate, A , B , N , M and C for the physical constraints and T_{melt} for the melting temperature, while T_0 for the alteration temperature. The typical temperature of it is 293-297 °K [33,35]. Table 3 shows the constraints of Johnson–Cook [35]. The options of crushable aluminium foam and its hardening

A Numerical Comparison between Aluminium Alloy And Mild Steel in Order to Enhance the Energy Absorption Capacity of the Thin Walled Tubes

possibilities in the usage of ABAQUS/Explicit software, are used in order to examine the plastic performance of the aluminium foam, follow the model of Dehspande and Fleck [36]. The yield condition of the model in question is as follows:

$$F = \hat{\sigma} - y \leq 0 \quad (9)$$

Where

$$\hat{\sigma}^2 = \frac{1}{[1+(\alpha/3)^2]} [\sigma_e^2 + \alpha \sigma_m^2] \quad (10)$$

Table 2: Mechanical properties of steel A36 material [26]

Factors	Value	Details
A	146.7 MPa	Material factor
B	896.9 MPa	Material factor
N	0.32	Coefficient of the strain power
C	0.033	Material factor
M	0.323	Power coefficient's temperature
ϵ^o	1.0 s ⁻¹	Reference strain value
ρ	7850 kg/m ³	Material density
T_m	1773 K	Temperature of melting
C_p	486 J/kg-1K	Specific heat

σ_e stands for the effective von Mises stress, σ_m for the mean stress, and Y for the yield strength [37]. α stands for the form of the yield surface, and is a task of ν_p , standing for the contraction's plastic constant, which is the rate of the plastic poisons of the aluminium foam material, with a presumed zero value [38, 39] as follows:

$$\alpha^2 = \frac{2(1-2\nu_p)}{9(1+\nu_p)} \quad (11)$$

In order to compute the strain hardening, the below calculation is integrated into the software:

$$Y = \sigma_p + \gamma \frac{\hat{\epsilon}}{\epsilon D} + \alpha_2 \ln \left[\frac{1}{1 - (\hat{\epsilon}/\epsilon D)^\beta} \right] \quad (12)$$

σ_p , stands for the plateau stress, α_2 , γ , ϵ_D and β represent the material property constants, while $\hat{\epsilon}$ stands for the effective strain. ϵ_D , standing for the densification strain, can be computed as below:

$$\epsilon_D = \frac{9 + \alpha^2}{3\alpha^2} \ln \left(\frac{\rho_f}{\rho_{fo}} \right) \quad (13)$$

ρ_f stands for the foam density, and ρ_{fo} for the base material's density [32,33]. The specifications of foam filler materials of the dynamic model are illustrated in Table 4[38].

Table 3: Specific specifications of the aluminium foam material [36]

ρ_f (kg/m ³)	σ_p (MPa)	α	α_2 (MPa)	β	γ	ϵ_D
540	12.56	2.12	1544	3.68	1	1.6206

Table 4: Specific specifications of the aluminium alloy material. [41]

ρ_f (kg/m ³)	σ_p (MPa)	E (GPa)	ν (ratio)
2700	235	68.3	0.3

B. Interaction, Boundary Conditions and Loading

During the experimentation one end of the rectangular profile is fixed to the rigid body (plate) by tied constraint, in order to allow only a linear movement lengthwise the displacement direction. The rotating motion of the nodes on the rectangular profile is allowed. The role of the rigid bodies as plates is to ease the contact simulation. One of the rigid bodies is fixed in order to allow only the axial movement of the compactor body. The mass is applied on one of the reference points in the centre of one moving plate, with defined velocity and mass compactor. The role of the reference point, located in the edge of the tube and the fixed plate, is to record the response. Step time with appropriate dynamic load, explicit action, and time period, which depends on the mesh dimension, and on the control and element structure, are specified by the program. The extended time interval requires more time to show the result and needs to have high CPU competency. The software ABAQUS/Explicit registers the interaction between all parts of the structure, like the contact between the walls and the aluminium foam, fixed plate, and the profile. The interaction is concluded once the contact surface is specified and the "penalty" of the friction coefficient is assigned. During the experimentation, the rectangular tube is fixed from both ends to the rigid body, in order to obtain their movement like one body. The mesh extension of the rectangular tube, having deformation length during the crush, was specified at 5mm size [27], [28].

IV. RESULT AND DISCUSSION

Tables 5 and 6 show the results of the investigation. The detailed description follows in the next subsections.

Table 5: Result of crashworthiness factors in case of rectangular model with various parameters (direct and oblique load) at length deformation of 200 mm in case mild steel

Indictors	Direct Load R- 300			Oblique Load R- 300		
	P max	CFE	Energy	P max	CFE	Energy
1.0 mm	129	0.27	7	80	0.32	5.14
1.2 mm	155	0.32	9.95	96.7	0.36	7
1.3 mm	168	0.33	11.3	106	0.39	8.2
2 mm	267	0.38	20.9	163	0.52	16.9

Table 6: Result of crashworthiness factors in case of rectangular model with various parameters (direct and oblique load) at length deformation of 200 mm in case aluminium alloy

Indictors	Direct Load R- 300			Oblique Load R- 300		
	P max	CFE	Energy	P max	CFE	Energy
1.5 mm	41.7	0.433	3.64	33	0.38	2.6
2.0 mm	58.4	0.43	5.07	45.7	0.47	4.3
3.0 mm	105	0.478	10.1	67.7	0.65	8.82
3.4 mm	126	0.5	12.68	76.5	0.7	10.9

A. Force displacement feature of different perimeter and thickness profile.

Figures 3 and 4 show the force displacement diagrams of the profile with 300 mm of perimeter, and the reaction of the different geometric profiles evoked by the direct and oblique load. Table 5 illustrate one type of perimeter 300 mm and four different thicknesses (1, 1.2, 1.3, and 2 mm), in case mild steel profile. Table 6 illustrate one type of perimeter 300 mm and four different thicknesses (1.5, 2, 3, and 3.4 mm) in case aluminium profile. Based on the results, the quantity of the absorbed energy is significantly higher in case if direct load. This is caused by the fact that the oblique load has the force of the axial compression and also of the bending mode, resulted by the progressive crush. The result of the force-displacement demonstrates that the various parameters don't have effect on the folding process during the crush of the rectangular tube, subjected to oblique and direct load. Both actions have same kind of results during the progressive collapse.

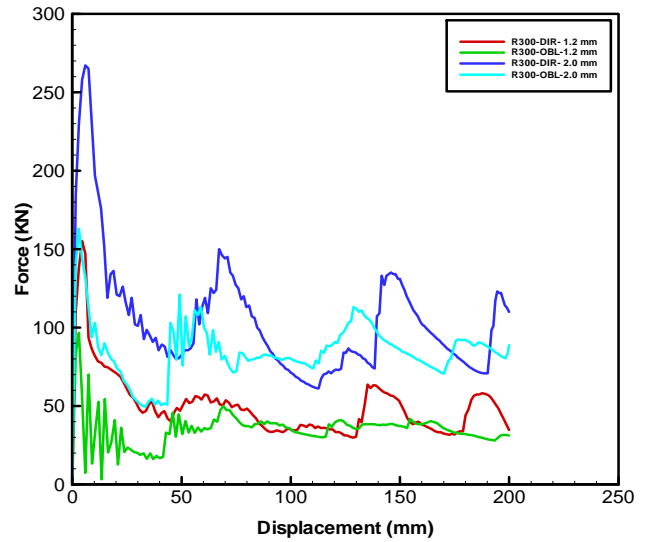


Fig.3. Force VS displacement for R-300 in case direct and oblique load to steel

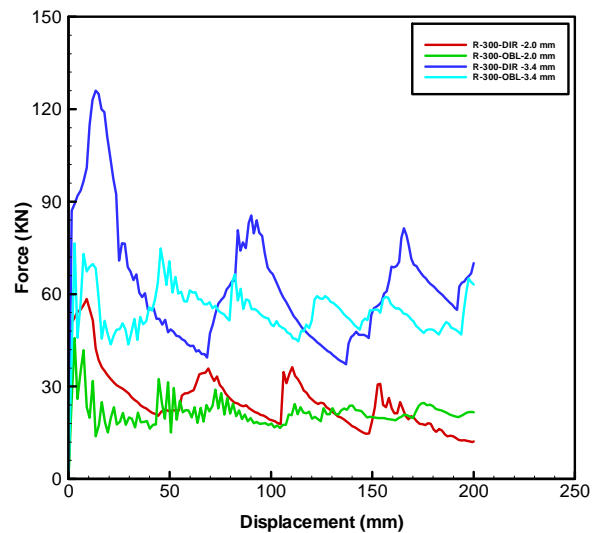


Fig.4. Force VS displacement for R-300 in case of oblique load to aluminium alloys

B. Energy Absorption

Figures 5 and 6 show the energy absorption capacity of the rectangular profile with 200 mm of deformation length, and with different thickness, subjected to various impact loads, and without concentrating on the time factor. As shown by the figures, in every impact condition, by increasing the thickness, proportionally increases the energy absorption capacity of the tube. Tables 5 and 6 show the energy absorption capacity of profiles with various thicknesses and perimeter 300 mm, in case of the direct and oblique load of 30 degrees. Based on the results, the tubes subjected to oblique load, had reduced energy absorption with a difference of 15 – 55 %. The optimal perimeter 300 mm and thickness of the tube need to be chosen based on the CFE, the energy absorption capabilities, fabrication process, and weight.

A Numerical Comparison between Aluminum Alloy And Mild Steel in Order to Enhance the Energy Absorption Capacity of the Thin Walled Tubes

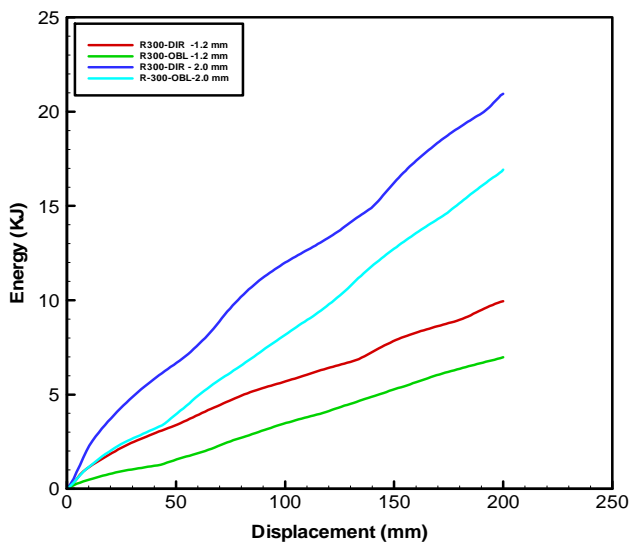


Fig.5. Energy VS displacement for R-300 in case direct and oblique load to steel

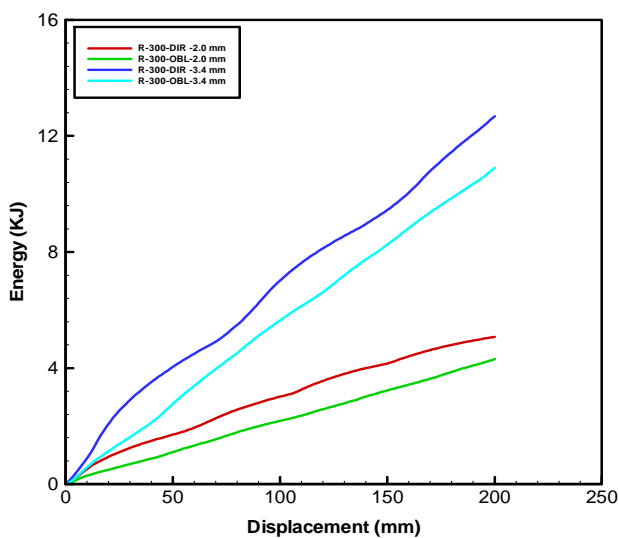


Fig.6. Energy VS displacement for R-300 in case direct and oblique load to aluminum alloy

C. Choice of the optimal profile

In this study the multi criteria decision making (MCDM) procedure is based on the complex proportional assessment method (COPRAS), which has the positive side of being convenient to handle. In case of the non-filled tubes, the 300 mm in diameter rectangular tube has the highest energy absorbing capability. In case of comparing the filled with the non-filled tubes, the rectangular profile of 300 mm in diameter filled with hollow aluminium foam has shown the best result in energy absorption capacity and crush force efficiency.

D. Influence of hollow foam on the capacity of energy absorption, peak force and CFE

The rectangular profile of 300 mm perimeter has been chosen for further examination regarding the wall thickness of the steel tube (1mm, 1.2mm, 1.3 mm and 2 mm) and (2, 2.4, 2.8, 3.2, and 3.4 mm) in case aluminium alloy tube, and the weight

of the hollow aluminium foam filling (A of 0.955kg, B of 0.9074kg, C of 0.841kg, D of 0.756kg, and E of 0.652kg). Figures 7, 8, 9, 10, 11, 12, 13, and 14 illustrates show the use of various weight of hollow aluminium foam, and wall thickness increases the CFE and energy absorption. Thinner tube has been chosen in order to keep the final design as low as possible, while increasing the absorber capability and the CFE. As illustrated in Tables 7-10, in case various wall thickness and 200 mm deformation length with hollow aluminium foam type (E), in case both mild steel and aluminium alloy profiles the enhancement of the energy absorption capacity and CFE Will be discussed in the next section.

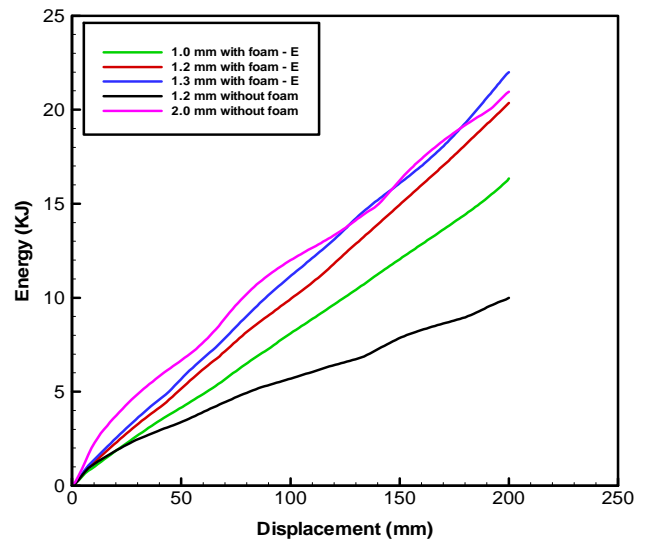


Fig.7. Effect of aluminium foam usage on the energy absorption under direct load of steel

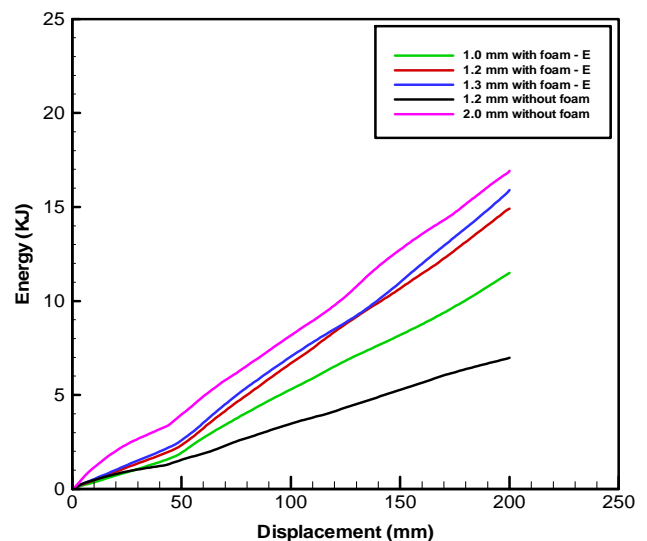


Fig.8. Effect of aluminium foam usage on the energy absorption under oblique load of steel

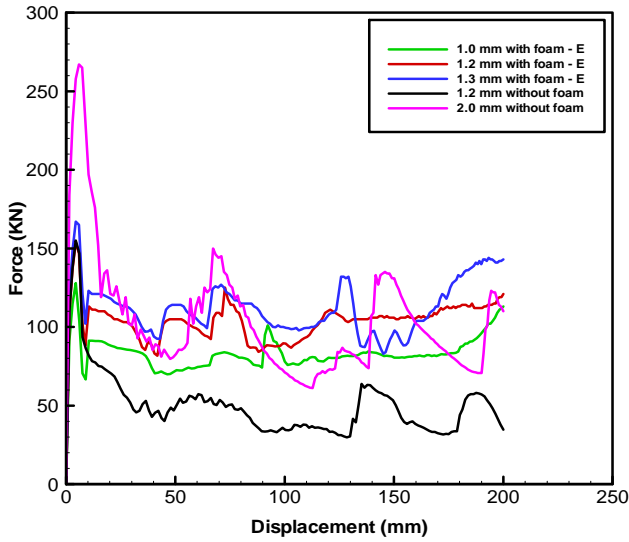


Fig.9. Effect of aluminium foam usage on the peak force under direct load of steel

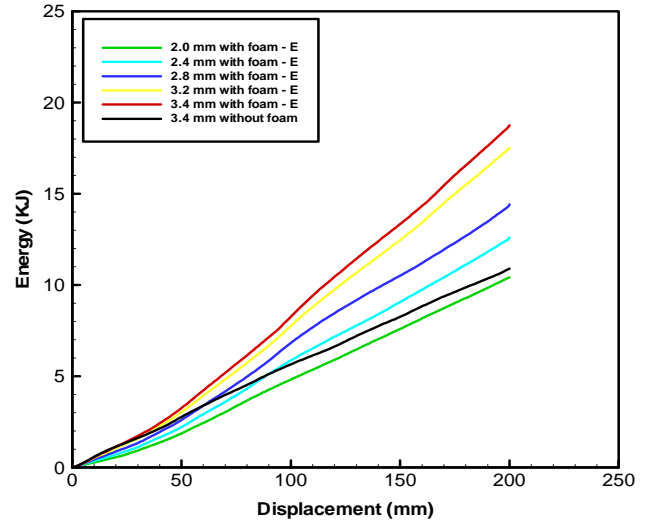


Fig.12. Influence of aluminium foam usage on the capacity of energy absorption under oblique load, in case of aluminum alloy

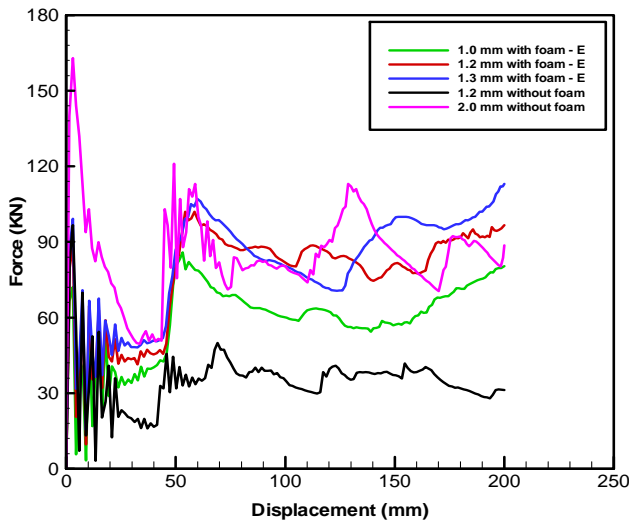


Fig.10. Influence of aluminium foam usage on the peak force under oblique loading of steel

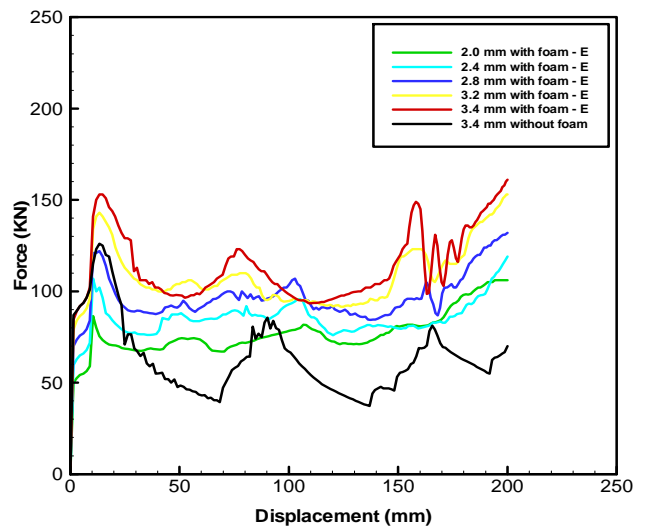


Fig.13. Effect of aluminium foam usage on the peak force under direct load of aluminum alloy

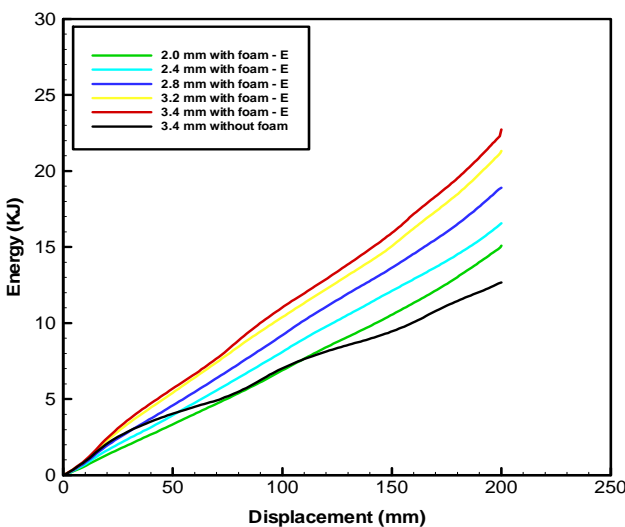


Fig.11. Effect of aluminium foam usage on the energy absorption under direct load of aluminum alloy

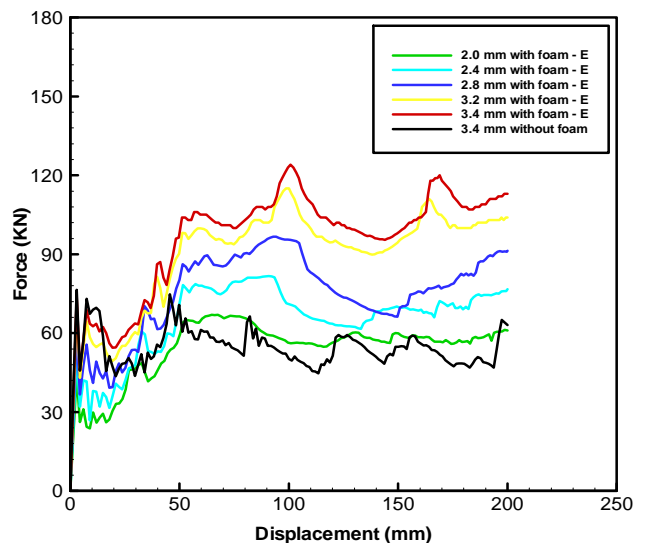


Fig.14. Influence of aluminium foam usage on the peak force when subjected to oblique load of aluminum alloy

E. Comprise between steel and aluminium alloy

1) Direct load

The simulations were based on the impact load applied to the rectangular profile of steel or aluminium material, in case direct load. The aluminium profile with hollow aluminium foam type (E) has a lower weight than the steel without foam or with foam with 2 mm and 1.2 mm of wall thickness of the steel respectively. The aluminium profile with 3.4 mm thickness and hollow aluminium foam has higher energy absorbing, peak force and CFE values, which are 22.4 KJ, 161 KN and 0.72 respectively. The steel profile with 1.2 mm thickness and hollow aluminium foam of the type (E) has more weight of the aluminium profile and less weight of steel profile without foam. The steel profile with aluminium foam has lower energy absorbing, peak force and CFE values of 20.4 KJ, 156 KN and 0.67 respectively. The steel profile with 2 mm thickness without aluminium foam has higher values than the steel profile with foam, and lower values then the aluminium profile with foam. Its weight is higher than the steel and aluminium profile with hollow aluminium foam. The steel profile has energy absorbing, peak force and CFD values of 20.9 KJ, 267 KN and 0.383 respectively. The optimal choice of rectangular tube is the aluminium rectangular profile of 3.4 mm thickness and hollow aluminium foam type (E), with enhancement of the energy absorption of 7.2 %, an improvement of CFE by 88%, decrease of peak force by 39.7 % and keeping the weight of final design at the lowest possible value. Figures 15 and 16, show the energy absorption and peak force at the same deformation length of 200 mm for both steel and aluminium profile.

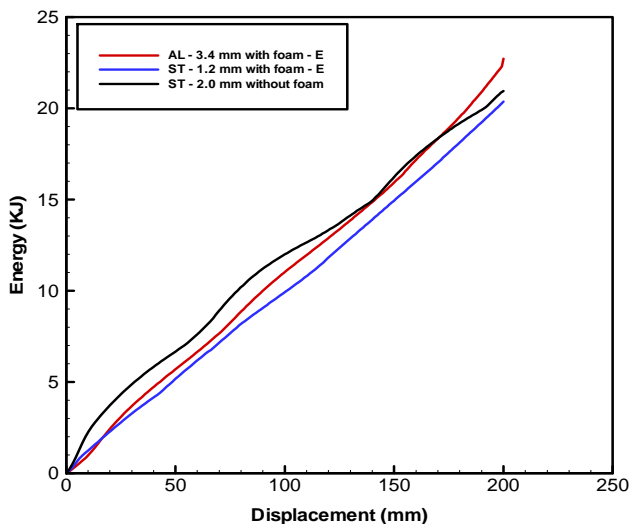


Fig.15. Show the difference of energy absorption between steel and aluminium alloy under direct impact load

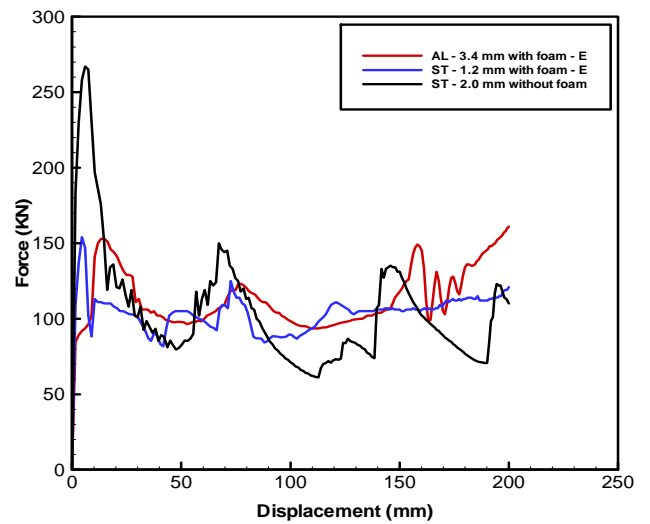


Fig.16. Shows the difference of peak force between steel and aluminium alloy under direct impact load

2) Oblique load

The simulations were based on an oblique lot of 30 degree applied to the rectangular profile of steel or aluminium material, in case oblique load. The aluminium profile with hollow aluminium foam type (E) has a lower weight than the steel without foam or with foam with 2mm and 1.2 mm of wall thickness of the steel respectively. The aluminium profile with 3.4 mm thickness and hollow aluminium foam has higher energy absorbing, peak force and CFE values of 18.9 KJ, 113 KN and 0.87 respectively. The steel profile with 1.2 mm thickness and hollow aluminium foam of the type (E) has more weight of the aluminium profile and less weight of steel profile without foam. The steel profile with aluminium foam has lower energy absorbing, peak force and CFE values of 15.9 KJ, 113 KN and 0.74 respectively. The steel profile with 2 mm thickness without aluminium foam has higher values than the steel profile with foam, and lower values than the aluminium profile with foam. Its weight is higher than the steel and aluminium profile with hollow aluminium foam. The steel profile has energy absorbing, peak force and CFD values of 17 KJ, 163 KN and 0.52 respectively. The optimal choice of rectangular tube is the aluminium rectangular tube of 3.4 mm thickness and hollow aluminium foam type (E), with enhancement of the energy absorption of 11.2 %, an improvement of CFE by 42.3%, decrease of peak force by 30.7 % and keeping the weight of final design at the lowest possible value. Figure 17 and 18, show the energy absorption and peak force at the same deformation length of 200 mm for both steel and aluminium profile.

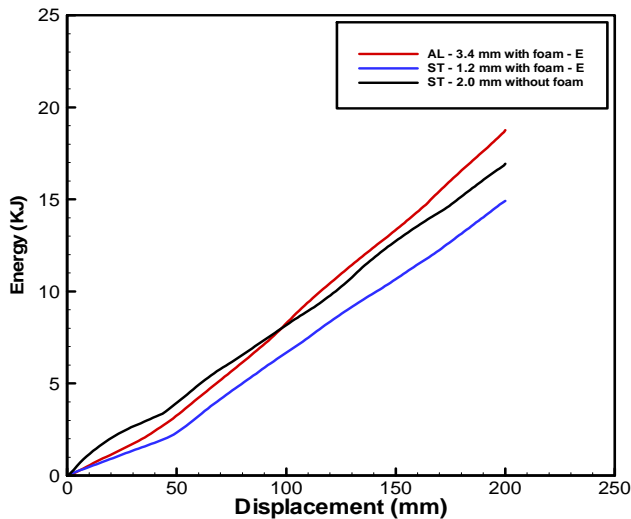


Fig.17. Show the difference of energy absorption between steel and aluminium alloy under oblique impact load

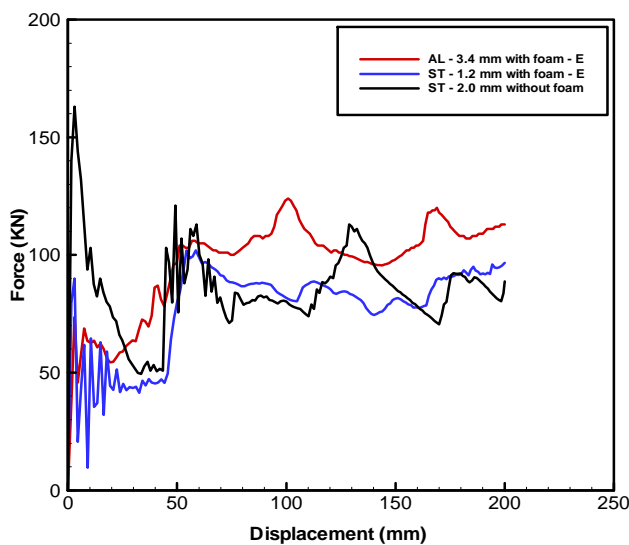
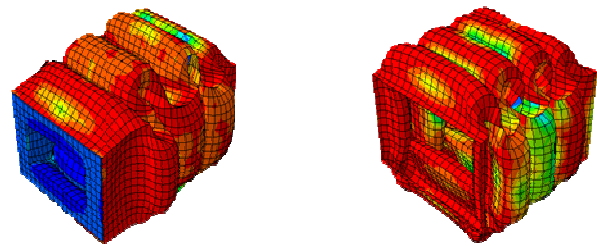


Fig.18. Shows the difference of peak force between steel and aluminium alloy under oblique impact load

V. CONCLUSION

The current study examined and comparison between the oblique and the direct impact loads, and the effects of the impact on the rectangular tube of ductile material of mild steel (A36) and aluminium alloy (AA6060). The purpose of the research was to choose the best from the different rectangular profiles with various thickness of tube and aluminium foam. The next step was to observe the behaviour of the chosen profile, filled with aluminium foam of various weights, and to discover the best filling option in case of direct and impact load. Another examined option of increasing the energy absorption, and the CFE was the usage if the trigger mechanism. The dynamic simulation was conducted with the compact mass of 25% of the total weight (1100 kg) of the passenger car, with impact speed of 15 m/s, and with both direct, and oblique load on the rectangular profile. Based on the crash performance indicators, cost and manufacturing practicality, The optimal choice of rectangular tube is the aluminium rectangular profile of 3.4 mm thickness and hollow aluminium foam type (E), under oblique load, with enhancement of the energy absorption of 11.2 %,

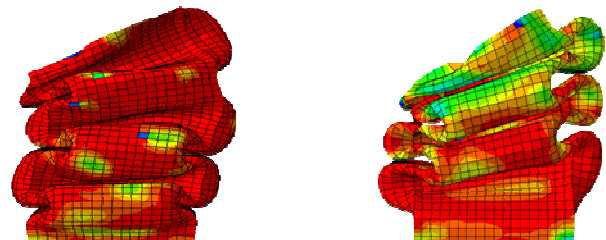
improvement of CFE by 42.3%, decrease of peak force by 30.7 % , in case the direct load, The optimal choice of rectangular tube is the aluminium rectangular profile of 3.4 mm thickness and hollow aluminium foam type (E), with enhancement of the energy absorption of 7.2 %, improvement of CFE by 88%, decrease of peak force by 39.7 % , and keeping the weight of final design at the lowest possible value. The best result has been given by the 3.4 mm thick rectangular aluminium alloy profile filled with hollow aluminium foam type E (0.652 kg), These profiles can be recognized as a potential energy absorber candidates for crashworthiness applications.



AL-Foam T= 3.4 mm

Al-Empty T= 3.4mm

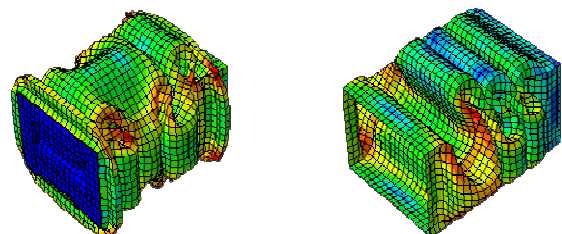
Fig.19. Crashing deformation longitudinal member, using different tube thicknesses with hollow aluminum foams E (0.652 Kg) for aluminum alloy under direct load



AL-Foam T= 3.4 mm

Al-Empty T= 3.4mm

Fig.20. Crashing deformation longitudinal member, using different tube thicknesses with hollow aluminum foams E (0.652 Kg) for aluminum alloy under oblique load

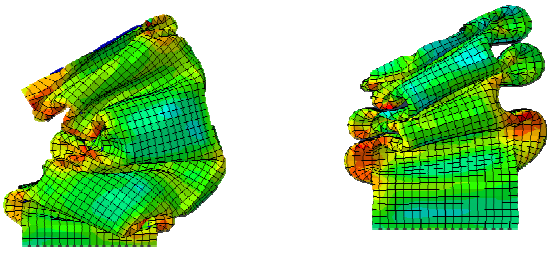


ST-Foam T= 1.2 mm

ST-Empty T= 2 mm

Fig.21. Crashing deformation longitudinal member, using hollow aluminum foams E (0.652 Kg) for mild steel under direct load

A Numerical Comparison between Aluminum Alloy And Mild Steel in Order to Enhance the Energy Absorption Capacity of the Thin Walled Tubes



ST-Foam T= 1.2 mm ST-Empty T= 2 mm

Fig.22. Crashing deformation longitudinal member, using hollow aluminum foams E (0.652 Kg) for mild steel under oblique load

Table 7: Effect of using different aluminum foam thickness and different tube thickness for R-300 subjected to direct loading, in case aluminium alloy.

Foam weight (Kg/mm ²)		A (0.955 Kg)			B (0.9074 Kg)			C (0.841 Kg)			D (0.756 Kg)			E (0.652 Kg)		
Thickn ess	Criteria	P max (KN)	CFE	Energy (KJ)	P max (KN)	CFE	Energy (KJ)	P max (KN)	CFE	Energy (KJ)	P max (KN)	CFE	Energy (KJ)	P max (KN)	CFE	Energy (KJ)
2 mm		250	0.57	25.4	232	0.59	24.5	144	0.77	20.9	128	0.79	19.2	106	0.73	15.1
2.4 mm		247	0.6	28	212	0.69	26.3	169	0.8	23.9	152	0.73	21.1	119	0.72	16.6
2.8 mm		X	X	X	X	X	X	155	0.84	24.7	166	0.75	23.5	132	0.74	18.9
3.2 mm		X	X	X	X	X	X	X	X	X	X	X	X	153	0.71	21.3
3.4 mm		X	X	X	X	X	X	X	X	X	X	X	X	161	0.72	22.4
Empty aluminum Tube thickness = 3.4 mm , Weight = 0.964 Kg														126	0.5	12.7

Note: X represents the design (tube + foam) which is above the intended weight.

Table 8: Effect of using different aluminum foam thickness and different tube thickness for R-300 subjected to oblique loading, in case aluminium alloy.

Foam weight (Kg/mm ²)		A (0.955 Kg)			B (0.9074 Kg)			C (0.841 Kg)			D (0.756 Kg)			E (0.652 Kg)		
Thickn ess	Criteria	P max (KN)	CFE	Energy (KJ)	P max (KN)	CFE	Energy (KJ)	P max (KN)	CFE	Energy (KJ)	P max (KN)	CFE	Energy (KJ)	P max (KN)	CFE	Energy (KJ)
2 mm		82.4	0.85	12.3	79.9	0.85	11.6	78.4	0.84	11.2	79.1	0.82	11.3	67	0.81	10.4
2.4 mm		96.6	0.86	14.4	97	0.84	14.2	96.3	0.83	14.3	93.7	0.80	14.3	81.7	0.80	12.6
2.8 mm		X	X	X	X	X	X	117	0.80	16.6	113	0.78	16.6	96.7	0.78	14.4
3.2 mm		X	X	X	X	X	X	X	X	X	X	X	X	115	0.80	17.5
3.4 mm		X	X	X	X	X	X	X	X	X	X	X	X	113	0.87	18.9
Empty aluminum tube thickness = 3.4 mm , Weight = 0.964 Kg														76.5	0.71	10.9

Note: X represents the design (tube + foam) which is above the intended weight.

Table 9: Effect of using different aluminium foam thicknesses, and tube thicknesses for R-300 subjected to direct load at length deformation of 200 mm, in case steel.

Foam weight (Kg/mm ²)	A (0.955 Kg)			B (0.9074 Kg)			C (0.841 Kg)			D (0.756 Kg)			E (0.652 Kg)			
Thickness	Criteria	P max (KN)	CFE	Energ y (KJ)	P max (KN)	CFE	Energ y (KJ)	P max (KN)	CFE	Energ y (KJ)	P max (KN)	CFE	Energ y (KJ)	P max (KN)	CFE	Energ y (KJ)
1 mm		X	X	X	X	X	X	X	X	X	157	0.72	21.4	128	0.65	16.3
1.2 mm		X	X	X	X	X	X	X	X	X	157	0.8	24.2	154	0.67	20.4
1.3 mm		X	X	X	X	X	X	X	X	X	176	0.75	25.5	167	0.672	22
Empty steel tube thickness = 2 mm , Weight = 1.638 Kg														267	0.38	20.9

Note: X represents the design (tube + foam) which is above the intended weight.

Table 10: Effect of using different aluminium foam thicknesses, and tube thicknesses for R-300 subjected to oblique load at length deformation of 200 mm. , in case steel.

Foam weight (Kg/mm ²)	A (0.955 Kg)			B (0.9074 Kg)			C (0.841 Kg)			D (0.756 Kg)			E (0.652 Kg)			
Thickness	Criteria	P max (KN)	CFE	Energ y (KJ)	P max (KN)	CFE	Energ y (KJ)	P max (KN)	CFE	Energ y (KJ)	P max (KN)	CFE	Energ y (KJ)	P max (KN)	CFE	Energ y (KJ)
1 mm		X	X	X	X	X	X	X	X	X	98	0.75	14	59.7	0.7	11.5
1.2 mm		X	X	X	X	X	X	X	X	X	113	0.72	15.8	102	0.76	14.9
1.3 mm		X	X	X	X	X	X	X	X	X	138	0.7	18.3	113	0.74	15.9
Empty steel tube thickness = 2 mm , Weight = 1.638 Kg														163	0.52	17

Note: X represents the design (tube + foam) which is above the intended weight.

ACKNOWLEDGMENT

The authors would like to thank Universiti Tenaga Nasional (UNITEN) and Ministry of water resources of Iraq for their generous support of the research projects that forms the basis for the current research.

REFERENCES

- [1]. Abramowicz, W., & Wierzbicki, T. (1988). Axial crushing of foam-filled columns. *International Journal of Mechanical Sciences*, 30(3), 263-271.
- [2]. Abramowicz, W., & Wierzbicki, T. (1989). Axial crushing of multicorner sheet metal columns. *Journal of Applied Mechanics*, 56(1), 113-120.
- [3]. Aktay, L., Toksoy, A. K., & Güden, M. (2006). Quasi-static axial crushing of extruded polystyrene foam-filled thin-walled aluminum tubes: experimental and numerical analysis. *Materials & design*, 27(7), 556-565.
- [4]. Chen, W., & Wierzbicki, T. (2001). Relative merits of single-cell, multi-cell and foam-filled thin-walled structures in energy absorption. *Thin-Walled Structures*, 39(4), 287-306.
- [5]. Hanssen, A. G., Hopperstad, O. S., Langseth, M., & Ilstad, H. (2002). Validation of constitutive models applicable to aluminium foams. *International journal of mechanical sciences*, 44(2), 359-406.
- [6]. Kavi, H., Toksoy, A. K., & Guden, M. (2006). Predicting energy absorption in a foam-filled thin-walled aluminum tube based on experimentally determined strengthening coefficient. *Materials & design*, 27(4), 263-269.
- [7]. Kim, H. S. (2002). New extruded multi-cell aluminum profile for maximum crash energy absorption and weight efficiency. *Thin-Walled Structures*, 40(4), 311-327.
- [8]. Santosa, S., & Wierzbicki, T. (1999). Effect of an ultralight metal filler on the bending collapse behavior of thin-walled prismatic columns. *International Journal of Mechanical Sciences*, 41(8), 995-1019.
- [9]. Seitzberger, M., Rammerstorfer, F. G., Gradinger, R., Degischer, H. P., Blaimschein, M., & Walch, C. (2000). Experimental studies on the quasi-static axial crushing of steel columns filled with aluminium foam. *International Journal of Solids and Structures*, 37(30), 4125-4147.
- [10]. Hanssen, A. G., Langseth, M., & Hopperstad, O. S. (1999). Static crushing of square aluminium extrusions with aluminium foam filler. *International Journal of Mechanical Sciences*, 41(8), 967-993.
- [11]. Hanssen, A. G., Hopperstad, O. S., & Langseth, M. (2000). Bending of square aluminium extrusions with aluminium foam filler. *Acta Mechanica*, 142(1-4), 13-31.
- [12]. Hanssen, A. G., Langseth, M., & Hopperstad, O. S. (2000). Static and dynamic crushing of square aluminium extrusions with aluminium foam filler. *International Journal of Impact Engineering*, 24(4), 347-383.
- [13]. Hanssen, A. G., Hopperstad, O. S., & Langseth, M. (2001). Design of aluminium foam-filled crash boxes of square and circular cross-sections. *International Journal of Crashworthiness*, 6(2), 177-188.
- [14]. Hanssen, A. G., Langseth, M., & Hopperstad, O. S. (2001). Optimum design for energy absorption of square aluminium columns with aluminium foam filler. *International Journal of Mechanical Sciences*, 43(1), 153-176.
- [15]. Song, H. W., Fan, Z. J., Yu, G., Wang, Q. C., & Tobota, A. (2005). Partition energy absorption of axially crushed aluminum foam-filled hat sections. *International Journal of Solids and Structures*, 42(9), 2575-2600.
- [16]. Chen, W. (2001). Optimisation for minimum weight of foam-filled tubes under large twisting rotation. *International Journal of Crashworthiness*, 6(2), 223-242.
- [17]. Chen, W., Wierzbicki, T., & Santosa, S. (2002). Bending collapse of thin-walled beams with ultralight filler: numerical simulation and weight optimization. *Acta mechanica*, 153(3-4), 183-206.
- [18]. Nariman-Zadeh, N., Darvizeh, A., & Jamali, A. (2006). Pareto optimization of energy absorption of square aluminium columns using multi-objective genetic algorithms. *Proceedings of the Institution of*



A Numerical Comparison between Aluminum Alloy And Mild Steel in Order to Enhance the Energy Absorption Capacity of the Thin Walled Tubes

- Mechanical Engineers, Part B: Journal of Engineering Manufacture, 220(2), 213-224.
- [19]. Zarei, H. R., & Kröger, M. (2007). Crashworthiness optimization of empty and filled aluminum crash boxes. *International Journal of Crashworthiness*, 12(3), 255-264.
- [20]. Zarei, H., & Kröger, M. (2008). Optimum honeycomb filled crash absorber design. *Materials & Design*, 29(1), 193-204.
- [21]. F. Tarlochan and Samer F. (2013). Design of thin wall structures for energy absorption applications: design for crash injuries mitigation using magnesium alloy. *IJRET*. 2 – (07)- 2319-1163.
- [22]. Cheng, Q., Altenhof, W., & Li, L. (2006). Experimental investigations of the crush behavior of AA6061-T6 aluminum square tubes with different types of through-hole discontinuities. *Thin-walled structures*, 44 (4), 441-454.
- [23]. Harte, A. M., Fleck, N. A., & Ashby, M. F. (2000). Energy absorption of foam-filled circular tubes with braided composite walls. *European Journal of Mechanics-A/Solids*, 19 (1), 31-50.
- [24]. Olabi, A. G., Morris, E., Hashmi, M. S. J., & Gilchrist, M. D. (2008). Optimized design of nested circular tube energy absorbers under lateral impact loading. *International Journal of Mechanical Sciences*, 50 (1), 104-116.
- [25]. Ahmad, Z., & Thambiratnam, D. P. (2009). Dynamic computer simulation and energy absorption of foam-filled conical tubes under axial impact loading. *Computers & Structures*, 87 (3), 186-197.
- [26]. Nagel, G. (2005). Impact and energy absorption of straight and tapered rectangular tubes (Doctoral dissertation, Queensland University of Technology).
- [27]. Nagel, G. M., & Thambiratnam, D. P. (2005). Computer simulation and energy absorption of tapered thin-walled rectangular tubes. *Thin-Walled Structures*, 43 (8), 1225-1242.
- [28]. Witteman, W. J. (1999). Improved vehicle crashworthiness design by control of the energy absorption for different collision situations: proefschrift. Technische Universiteit Eindhoven.
- [29]. Dehghan-Manshadi, B., Mahmudi, H., Abedian, A., & Mahmudi, R. (2007). A novel method for materials selection in mechanical design: combination of non-linear normalization and a modified digital logic method. *Materials & design*, 28(1), 8-15.
- [30]. Olabi, A. G., Morris, E., Hashmi, M. S. J., & Gilchrist, M. D. (2008). Optimised design of nested circular tube energy absorbers under lateral impact loading. *International Journal of Mechanical Sciences*, 50(1), 104-116.
- [31]. Witteman, W. J. (1999). Improved vehicle crashworthiness design by control of the energy absorption for different collision situations: proefschrift. Technische Universiteit Eindhoven.
- [32]. Ahmad, Z., & Thambiratnam, D. P. (2009). Dynamic computer simulation and energy absorption of foam-filled conical tubes under axial impact loading. *Computers & Structures*, 87(3), 186-197.
- [33]. Duan, C. Z., Dou, T., Cai, Y. J., & Li, Y. Y. (2011). Finite element simulation and experiment of chip formation process during high speed machining of AISI 1045 hardened steel. *AMAE International Journal on Production and Industrial Engineering*, 2(1).
- [34]. Dean, J., Dunleavy, C. S., Brown, P. M., & Clyne, T. W. (2009). Energy absorption during projectile perforation of thin steel plates and the kinetic energy of ejected fragments. *International journal of impact engineering*, 36(10), 1250-1258.
- [35]. Lacy, J. M., Shelley, J. K., Weathersby, J. H., Daehn, G. S., Johnson, J., & Taber, G. (2010, October). Optimization-based constitutive parameter identification from Sparse Taylor cylinder data. In *Proceedings of the 81st shock and vibration symposium*. Idaho National Laboratory, US.
- [36]. Deshpande, V. S., & Fleck, N. A. (2000). Isotropic constitutive models for metallic foams. *Journal of the Mechanics and Physics of Solids*, 48(6), 1253-1283.
- [37]. Shahbeyk, S., Petrinic, N., & Vafai, A. (2007). Numerical modelling of dynamically loaded metal foam-filled square columns. *International journal of impact engineering*, 34(3), 573-586.
- [38]. Ahmad, Z., & Thambiratnam, D. P. (2009). Dynamic computer simulation and energy absorption of foam-filled conical tubes under axial impact loading. *Computers & Structures*, 87(3), 186-197.
- [39]. Reyes, A., Hopperstad, O. S., Berstad, T., Hanssen, A. G., & Langseth, M. (2003). Constitutive modeling of aluminum foam including fracture and statistical variation of density. *European Journal of Mechanics-A/Solids*, 22(6), 815-835.
- [40]. Tarlochan, F., Samer, F., Hamouda, A. M. S., Ramesh, S., & Khalid, K. (2013). Design of thin wall structures for energy absorption applications: Enhancement of crashworthiness due to axial and oblique impact forces. *Thin-Walled Structures*, 71, 7-17.
- [41]. Jensen, Ø., Langseth, M., & Hopperstad, O. S. (2004). Experimental investigations on the behaviour of short to long square aluminium tubes subjected to axial loading. *International Journal of Impact Engineering*, 30(8), 973-1003.

AUTHORS

Jamal O. Sameer was born in Iraq. He obtained his Bachelors in Mechanical Engineering from Iraq. He is currently pursuing his Master of Mechanical Engineering in the field of applied Mechanical Engineering at Universiti Tenaga Nasional (UNITEN), Kajang, Selangor, Malaysia.



Omar S. Zarooq . Mechanical Engineer, He obtained his PHD in Mechanical Engineering from UPM. He is currently an Dr. lecturer at Univirsiti of Tenaga Nassional / College of Engineering / Kuala Lumpur, Malaysia



Samer F. Was born in Iraq. He obtained his Bachelors in Mechanical Engineering and Master in Mechanical Engineering from Iraq. He obtained his PHD in Mechanical Engineering from UNITEN, Malaysia. He is a lecturer at College of Engineering, Alanbar University, Iraq.



Abdulbasit Abdullah was born in Iraq. He obtained his bachelors in General of Mechanical Engineering from Iraq. He is currently pursuing his Master of Mechanical Engineering in the field of applied Mechanical Engineering at Universiti Tenaga Nasional (UNITEN), Kajang, Selangor, Malaysia.

